SCIENTIA PLENA
www.scientiaplena.org.br
VOL. 21, NUM. 07 2025
doi: 10.14808/sci.plena.2025.074201

Acetonitrile combustion over (Cu, Co, Fe)-Beta catalysts

Combustão de acetonitrila sobre catalisadores (Cu, Co, Fe)-Beta

B. C. S. Silveira; M. S. Batista*

Departamento de Engenharia Química, Universidade Federal de São João del Rei, 36497-899, Ouro Branco-MG, Brasil

**marcelobatista@ufsj.edu.br*
(Recebido em 15 de outubro de 2024; aceito em 03 de julho de 2025)

Acetonitrile is a volatile organic compound (VOC) commonly found in off-gas from industrial processes that have low activity, high stability, and toxicity which cause continuous damage to human and animal health and the atmospheric environment. In this paper was evaluate the performance of (Cu, Co or Fe)-Beta catalysts in the acetonitrile combustion varying the reaction temperature. (Cu, Co or Fe)-Beta catalysts were prepared by ion exchange method and characterized by X-ray fluorescence (XRF), X-ray diffractometry (XRD), temperature-programmed reduction by hydrogen (H2-TPR) and UV-VIS spectroscopy. The results showed the presence of Cu2+ ions and CuO nanoparticles in Cu-Beta, as well as Fe2O3 and Fe3+ in Fe-Beta. Co2+ species are in position of load compensation in the Beta zeolite and has no shown reduction peak. On the other hand, the reduction occurred in more than one stage in the (Cu and Fe)-Beta catalysts. Acetonitrile conversion increased with increasing reaction temperature and the order of activity was Cu-Beta > Fe-Beta > Co-Beta. Fe-Beta led to the formation of HCN, NH3, N2 and N2O+NO, while Co-Beta led to the formation of N2 and N2O+NO. Cu-Beta catalyst was the most active and highly selective to N2. The excellent performance of Cu-Beta was attributed to the co-existence of both highly dispersed CuO nanoparticles and Cu2+ species.
Keywords: acetonitrile, pollution, catalytic combustion.

Acetonitrila é um composto orgânico volátil (COV) comumente encontrado em gases de escape de processos industriais que apresentam baixa atividade, alta estabilidade e toxicidade que causam danos contínuos à saúde humana e animal e ao ambiente atmosférico. Neste trabalho foi avaliado o desempenho de catalisadores (Cu, Co ou Fe)-Beta na combustão de acetonitrila variando a temperatura de reação. Catalisadores de (Cu, Co ou Fe)-Beta foram preparados pelo método de troca iônica e caracterizados por fluorescência de raios X (XRF), difratometria de raios X (DRX), redução a temperatura programada por hidrogênio (H2-TPR) e espectroscopia no UV-VIS. Os resultados mostraram a presença de íons Cu2+ e nanopartículas de CuO em Cu-Beta, bem como Fe2O3 e Fe3+ em Fe-Beta. As espécies Co2+ estão em posição de compensação de carga na zeólita Beta e não apresentaram pico de redução. Por outro lado, a redução ocorreu em mais de uma etapa nos catalisadores (Cu e Fe)-Beta. A conversão de acetonitrila aumentou com o aumento da temperatura de reação e a ordem de atividade foi Cu-Beta > Fe-Beta > Co-Beta. Fe-Beta levou à formação de HCN, NH3, N2 e N2O+NO, enquanto Co-Beta levou à formação de N2 e N2O+NO. O catalisador Cu-Beta foi o mais ativo e altamente seletivo a N2. O excelente desempenho do Cu-Beta foi atribuído à coexistência de nanopartículas de CuO altamente dispersas e espécies de Cu2+.
Palavras-chaves: acetonitrila, poluição, combustão catalítica.

1. INTRODUCTION

Currently, there has been an increasing attention to the environmental protection subject, especially the purification of toxic air pollutants [1-3]. Among the various gaseous pollutants, N-containing exhaust gases, such as acrylonitrile (C_2H_3CN), acetonitrile (CH_3CN), and hydrocyanic acid (HCN), ammonia (NH_3) and nitric oxides (NO_x), can lead to seriously environmental problems because of their hazardous properties. They are usually classified as volatile organic compounds (VOCs) [4-5]. Acetonitrile is an organic compound predominantly emitted from the burning of biomass and from the industrial production of various chemicals and polymers [6-7]. For the treatment of this pollutant is traditionally used thermal combustion. However, this method requires high temperatures (above 1000 °C) which means high energy demand and leads to secondary pollution by the formation of nitrogenous products (NOx) [8]. The danger of acetonitrile and secondary pollutants makes it necessary to search for more efficient treatments.

Selective catalytic combustion (SCC) emerges as an interesting alternative due to the lower reaction temperature associated (low operation cost) with greater formation of products of interest such as N_2 and CO_2 [9-10]. However, the challenge is to find the most suitable catalyst for the catalytic combustion of acetonitrile.

Zhang et al. (2014) [11] studied metal-modified mesoporous materials (Cu, Co, Fe, V, Mn, Pd, Ag and Pt) as catalysts for acetonitrile combustion. Noble metals (Pt, Pd, Rh) exhibited low-temperature activity, but lead to harmful by-products (NO, NO_2, N_2O, NH_3, and CO), which are undesirable. On the other hand, transition metal catalysts such as copper, cobalt and iron exhibited promising results. Nanba et al. (2004) [12] found that Cu/HZSM-5 could completely convert acrylonitrile with N_2 selectivity of around 80% at temperatures above 350 °C. This better result was associated with the redox property and the presence of isolated Cu^{2+} species. However, the metal-support interaction modifies the redox property and N_2 selectivity of catalysts. Wang et al. (2020) [13] showed that the introduction of strongly acidic support significantly limited the formation of NOx and improved the N_2 selectivity. NOx originating from over-oxidation on metal oxides could be reduced by NH_3 derived from the acetonitrile hydrolysis reaction on acidic sites of zeolites. Therefore, the synergism metal-support is crucial to both high activity and N_2 selectivity. Moreover, both highly dispersed oxides and ionic species exchanged in zeolite would be beneficial to superior catalytic activity [14].

Additionally, Beta zeolite was employed herein as strongly acidic support to facilitate the transition metal dispersion and hydrolysis process due to their advantages of high specific surface areas, abundant acidic sites and good thermal stabilities [15-17]. Transition metals such as copper, cobalt and iron are preferred due to their low cost, thermal stability and a satisfactory activity and selectivity in reactions with nitrogen compounds [10, 18-19].

In this paper, the performance of acetonitrile combustion (including the activity, monitoring of CO_2 and N-containing by-product) over (Cu, Co or Fe)-Beta catalysts prepared by the ion exchange method were investigated. To do this, various characterization studies by X-ray diffraction (XRD), X-ray fluorescence (XRF), temperature programmed-reduction by hydrogen (H_2-TPR) and UV-VIS spectroscopy were performed to reveal the reaction behaviours of acetonitrile catalytic combustion.

2. MATERIAL AND METHODS

2.1 Catalyst preparation

(Cu, Co, Fe)-Beta catalysts were prepared by ion-exchange methods using commercial NH_4-Beta zeolite (TRICAT, Si/Al=12). High purity reagents (99%) were used, as well as care for cleaning materials to avoid contamination and consequently distorted results. For each catalyst, 4 g of zeolite was exchanged three times with aqueous solutions (0.1 mol/L) of cupric, cobalt (II) and ferric nitrates at room temperature using 50 mL of solution per gram of zeolite for 12 h each exchange. After each step, the mixture was filtered and the retained solid was washed with distilled water and dried at 110 °C for 2 h. This procedure was performed three times, and then the solid was calcined in muffle at 650 °C (10°C/min) during 2 h to obtain the (Cu, Co, Fe)-Beta catalysts.

2.2 Catalyst characterization

The catalysts were characterized by X-ray fluorescence (XRF), X-ray diffractometry (XRD), temperature-programmed reduction by hydrogen (H_2-TPR) and UV-VIS spectroscopy.

XRF analyses were carried out in equipment Shimadzu EDX 720/800HS with 200 mg of catalyst in air atmosphere and flow of 200 mL/min of helium gas. Internal calibration was used in the analyses.

XRD analyses were performed by the powder method using a Rigaku diffractometer (Miniflex 600) with Cu tube, Ni-filtered, operating at 40 KV, 15 mA and CuKα radiation. The scanning

speed was 2º(2θ)/min and the angle ranging between 5 and 80º(2θ). H_2-TPR analyses were performed on SAMP3 apparatus (Termolab Equipment, Brazil) equipped with a thermal conductivity detector (TCD). A trap was used to remove the water stemming from the reduction before the gas of the reactor outlet was sent to the TCD. TPR started with a ramp of 10 °C/min from 100 °C until 1000 °C. It is worth noting that the TPR peaks are wide when using heating ramp with lower rates, on the other hand, the peaks can come together when using ramp with higher rates. A flow of 30 mL/min from a high purity mixture of 2 % H_2 in argon gas and 100 mg of sample were used. The use of smaller flows may be limited by mass transfer, on the other hand, larger flows increase gas consumption and may lead to catalyst sample carryover.

The diffuse reflectance spectra were recorded with a UV–VIS spectrophotometer (Shimadzu UV 2700). $BaSO_4$ was used as reference material. Before the measurement, the samples were dried at 120 °C for 2 h to remove the water or OH groups. Samples were scanned in the range of 200–800 nm. The reflectance data were converted to the Schuster-Kubella-Munk function, $F(R) = (1 - R)^2 / 2R$, where R is the diffuse reflectance obtained directly from the spectrometer.

2.3 Catalytic reaction

The catalysts were evaluated in the combustion reaction of acetonitrile using a quartz wool-type "U" reactor and 8.6 mg of metal (copper, cobalt or iron) in the sample, fed with continuous flow of 50 mL/min of a mixture containing 2.8 vol.% acetonitrile (CH_3CN) in synthetic air. The reactor was operated at atmospheric pressure and the reaction temperature was varied from 100 to 600 °C (based on preliminary data). The reactor was coupled in line to a mass spectrometer (THERMO) for gas analysis: N_2 (m/z = 28), O_2 (m/z = 32 and 16), NO + N_2O (m/z = 30), NO_2 (m/z = 46), NH_3 (m/z = 17), HCN (m/z = 27), CH_3CN (m/z = 41) and CO_2 (m/z = 44). Conversion of CH_3CN was calculated through Equation 1.

$$Conversion\ (\%) = \left(\frac{CH_3CN_{(in)} - CH_3CN_{(out)}}{CH_3CN_{(in)}}\right) \times 100 \quad (1)$$

Where $CH_3CN_{(in)}$ is the molar flow rate of the introduced reagent, and $CH_3CN_{(out)}$ is the molar flux rate of the corresponding composition in the effluent.

3. RESULTS AND DISCUSSION

Figure 1 shows the X-ray diffraction patterns of Cu-Beta, Fe-Beta and Co-Beta catalysts and NH_4-Beta zeolite. All samples presented the characteristic peaks of BEA crystalline structures at 2θ = 7.6° and 22.3° (PDF#48-0074). BEA crystalline structure was well preserved even after ionic exchange and calcination. In addition, Cu-Beta and Fe-Beta showed also peaks belonging to CuO at 2θ= 35.5, 38.7, 48.7° and Fe_2O_3 at 2θ = 33.2°, 35.6°, 40.9°, 49.5°, respectively. This indicates that during the ionic exchange occurred precipitation, and after calcination, decomposition of $Cu(OH)_2$ to tenorite CuO which belongs to the monoclinic crystal system (PDF#41-0254) and $Fe(OH)_3$ decomposition to hematite α- Fe_2O_3 (PDF#01-1053). In addition, the calcination temperature leads to phase changes, it can also cause changes in the crystallography, microstructure and grain size crystals [20].

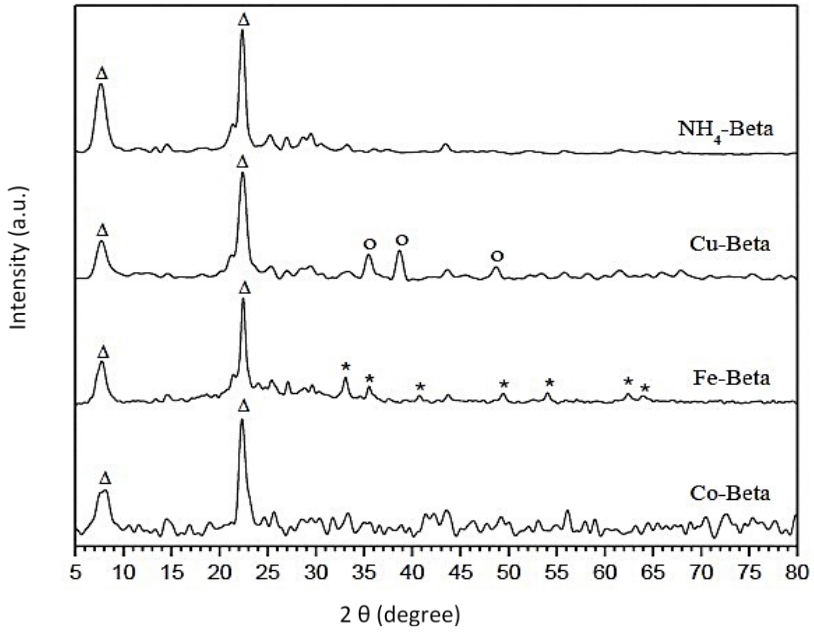

Figure 1: NH_4-Beta, Cu-Beta, Fe-Beta and Co-beta samples diffractogram, where (Δ) corresponds to the zeolite peaks, (○) to the CuO peaks and (*) to the Fe_2O_3 peaks.

However, Co-BETA no exhibited cobalt oxides characteristic peaks. The absence of oxide peaks indicates that the cobalt species are mainly exchanged in the Beta zeolite structure [21]. No characteristic peak pattern of CoO and Co_3O_4 was also observed by other authors [22]. According to the values of the solubility product constants (K_{SP}), they are more susceptible to precipitation of $Fe(OH)_3$ ($K_{SP}=2.79\times10^{-39}$, 25°C) and $Cu(OH)_2$ ($K_{SP}=1\times10^{-19.7}$, 25°C), than $Co(OH)_2$ ($K_{SP}=6.32\times10^{-15}$, 25°C) [23, 24]. In (Cu, Co, Fe)-Beta catalysts, information about the crystalline phase and its stability can provide a more solid basis for understanding catalyst performance.

Table 1 shows the average size of the crystallites of (Cu, Co, Fe)-Beta catalysts and Beta zeolite calculated by the Debye-Scherrer equation. Note that the size of CuO crystallites is close to Beta zeolite crystallites, indicating that the oxide particles are possibly dispersed over the outer surface of Cu-Beta. On the other hand, Fe-Beta crystallite was increased to 32.2 nm and Fe_2O_3 has an average size of 22 nm. This suggests that an iron oxide layer may have formed on the external surface of the zeolite crystallites, which would have led to an increase in Fe-Beta crystallite when compared to Beta zeolite [25-26].

Table 1: Average crystallite size of (Cu, Co, Fe)-Beta and NH_4-Beta samples.

Samples	Metal content [a] (wt. %)	Crystal size [b] (nm)	Degree of reduction [c] (α)
NH_4-Beta	-	21	-
Cu-Beta	19.7	20	0.99
Fe-Beta	7.3	32	0.54
Co-Beta	5.8	21	-

[a]Obtained by X-ray fluorescence (XRF). [b]Average particle size calculated by the Debye-Scherrer equation using reflection of CuO (2θ = 38.7°) and Fe_2O_3 (2θ = 33.2°). [c]Ratio between moles of H_2 consumed/moles of metal.

TPR-H_2 profiles of (Cu, Fe, Co)-Beta catalysts are shown in Figure 2. Cu-Beta has two reduction peaks which indicate a reduction in more than one step. The first peak at 229 °C corresponds to the reduction of $Cu^{2+} \rightarrow Cu^{+}$ and nanoparticles of $CuO \rightarrow Cu^0$, and the second peak at 356 °C was attributed to the successive reduction of $Cu^{+} \rightarrow Cu^0$ [27]. Fe-Beta has three peaks of reduction. The first peak corresponds to the reduction of Fe_2O_3 to Fe_3O_4, which occurs

at 407 °C [28]. The second peak at 445 °C was attributed to the reduction of $Fe^{3+} \rightarrow Fe^{2+}$, in exchange position at the Brönsted sites, and the reduction of Fe_2O_3 remaining in Fe_3O_4 [29]. The third peak at 616 °C occurred the reduction of $Fe_3O_4 \rightarrow Fe^0$, which can occur directly or with FeO as an intermediate ($Fe_3O_4 \rightarrow FeO \rightarrow Fe^0$). The reduction of Fe^{2+} in the exchange position for Fe^0 was not observed, which requires temperatures above 1000 °C and occurs together with the destruction of the zeolite structure [30-32]. Note that the Co-Beta catalyst did not show any reduction peak, corroborating to the result observed by XRD that indicated the absence of cobalt oxide. The absence of reduction peaks indicates that cobalt is in ion exchange position under strong interaction with the Beta zeolite structure [33].

Table 1 showed the total hydrogen consumption of H_2/M molar ratio. Cu-Beta showed a ratio near to 1, which is according to the theoretical value for the reduction of Cu^{2+} to Cu^0 [28]. Copper content on Cu-Beta exceeds the entire ion exchange capacity of the Beta zeolite. The Si/Al ratios of the Beta zeolite predict the maximum amount of copper is 3.9 wt.%, considering that one Cu^{2+} cation needs two ionic exchange sites. In this way, considering the ratio of areas under the peaks in Figure 2, we arrive at the estimation for the distribution of the exchangeable Cu-species prior to reduction for Cu-Beta. This analysis showed that 85% of the copper in Cu-Beta are CuO nanoparticles. On the other hand, Fe-Beta exhibited inferior ratios obtained that can be associated to Fe^{2+} exchange (after Fe^{3+} reduction) which is not capable of reducing completely to metallic state without the collapse of the zeolitic structure. It can explain the iron catalysts showing an H_2/Fe ratio below 1.5 [29].

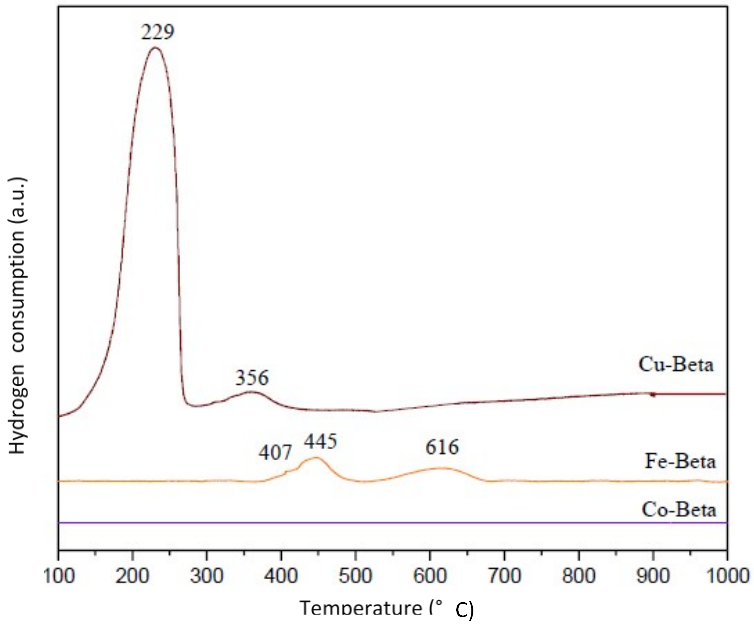

Figure 2: TPR-H_2 profiles of Cu-Beta, Fe-Beta and Co-Beta catalysts.

The further information of the species on the (Cu, Fe, Co)-Beta catalysts were studied by UV-VIS spectroscopy, as shown in Figure 3. Cu-Beta showed bands between 200-250 nm correspond to Cu-O charge transfer (CT) transition. The bands at 212 and 244 nm can be associated to Cu^{2+} exchanged as a single site on zeolite structure [34]. Additionally, a broad absorption in the region of d–d transitions at 400-800 nm of the octahedral Cu^{2+} in crystalline structure of CuO nanoparticles [35]. Fe-Beta shows the bands at 217, 272, 370, 482 nm. The bands at 217 and 272 nm were assigned to CT transitions of the octahedral Fe^{3+} ions. The band at 370 nm was associated with CT transitions of FeOx species. The band at 482 nm was related to d-d transitions of Fe_2O_3 nanoparticles [36]. Co-Beta showed bands between 200-250 nm attributed to CT transition between cobalt ion and oxygen. Finally, bands in the 400-700 nm range

have been attributed to d-d transitions of octahedral Co^{2+} ions [37]. These results are consistent with the XRD and TPR measurements of these catalysts.

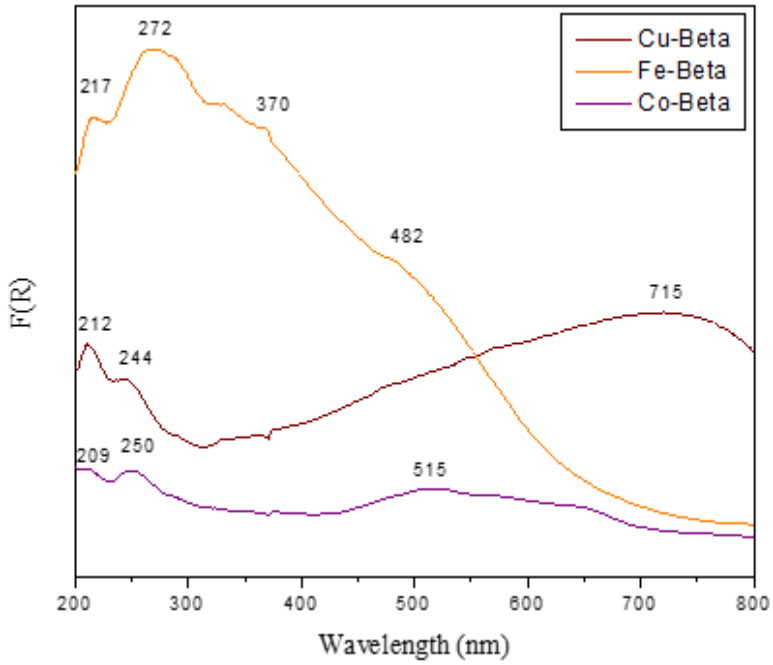

Figure 3: UV-VIS spectra of (Cu, Fe, Co)-Beta catalysts.

The results of CH_3CN conversion on (Cu, Fe, Co)-Beta catalysts as a function of reaction temperature are showed in Figure 4. Beta zeolite only has practically no activity under the conditions studied (no shown). Therefore, copper, cobalt and iron species are active sites for the acetonitrile combustion. It was found that the acetonitrile initial conversion rises rapidly upon the temperature and almost keeps stable at a temperature range of 450–600 °C on all catalysts. Cu-Beta has the highest activity at low temperature and the superior performance was attributed to the co-existence of highly dispersed copper oxide and Cu^{2+} exchanged species. Furthermore, Cu-Beta showed a very stable conversion rate with a 10 h reaction time (no showed). In Fe-Beta were identified octahedral Fe^{3+} ions and Fe_2O_3 nanoparticles, which contributed to the second-best catalytic activity. On the other hand, Co-Beta had the lowest activity among the studied catalysts. No cobalt oxide was observed in the XRD and TPR analyses, which indicates the presence of Co^{2+}-exchanged species in the zeolite structure. The Co^{2+} species at the ion exchange sites should only be reduced at high temperatures [32, 38]. Therefore, Co-Beta activity for the acetonitrile combustion tends to be reduced due to its limited redox properties [39].

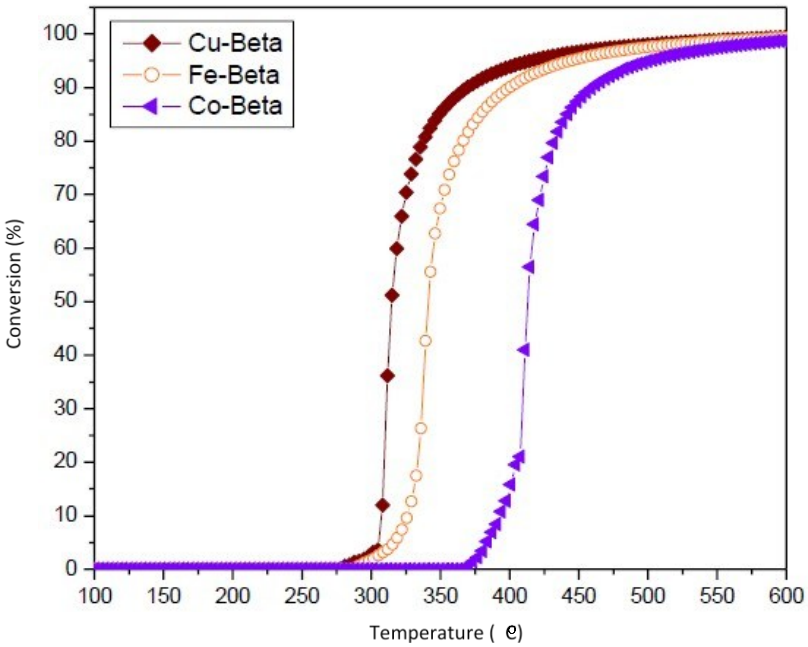

Figure 4: Combustion of acetonitrile over Cu-Beta, Fe-Beta and Co-Beta catalysts.

Figure 5 shows the product streams formed on the (Cu, Fe, Co)-Beta catalysts. During catalytic combustion, the following compounds were identified: NH_3, HCN, NO_2, NO, N_2O and CO_2. Note that Cu-Beta presented practically the products of interest such as CO_2 and N_2 (Fig. 5a). Cu-Beta shows a rapid increase in CO_2 formation at 300 °C, followed by N_2 formation at 325 °C. Figure 5b shows the products formed on Fe-Beta. Note the formation of CO_2 at 285 °C, N_2 and NH_3 at 340 °C, as well as the formation of HCN at 325 °C. The increase in temperature favored the consumption of HCN and NH_3, while it increased the formation of N_2 and N_2O+NO. However, Co-Beta showed the formation of N_2O+NO between 500-550 °C, as well as CO_2 and N_2 at approximately 340 °C and 425 °C, respectively (Figure 5c). These results suggested different reaction pathways for Fe-Beta and (Co, Cu)-Beta [40]. Cu-Beta and Co-Beta followed an oxidation pathway ($CH_3CN \rightarrow NCO \rightarrow N_2/NOx, CO_2$), while Fe-Beta proceeded via hydrolysis pathway ($CH_3CN \rightarrow CH_3CONH_2 \rightarrow HCN, NH_3$) [41-43]. However, the increase in temperature favored the consumption of HCN and NH_3 or change of reaction pathway increasing the formation of N_2 and N_2O + NO on Fe-Beta. On the other hand, Cu^{2+} exchanged Beta zeolite would be beneficial to N_2 selectivity due to the improved internal SCR (Selective Catalytic Reduction) reaction to reduce NOx from oxidation pathways [42]. Additionally, the carbonaceous species like NCO and CO were more easily oxidated to CO_2 on the Cu-Beta.

Overall, it could be concluded that Cu-Beta had the highest conversion and the highest formation of products of interest. Fe-Beta showed lower conversion than Cu-Beta and led to the formation of NH_3, HCN and N_2O+NO. This result makes its use not interesting, mainly due to the dangerous nature of the formed compounds. Among the catalysts, Co-Beta had the lowest activity and led to the formation of N_2O+NO. However, the catalytic activity of cobalt-based catalysts can be improved by enhancing their redox process, for example by using Co_3O_4 [39].

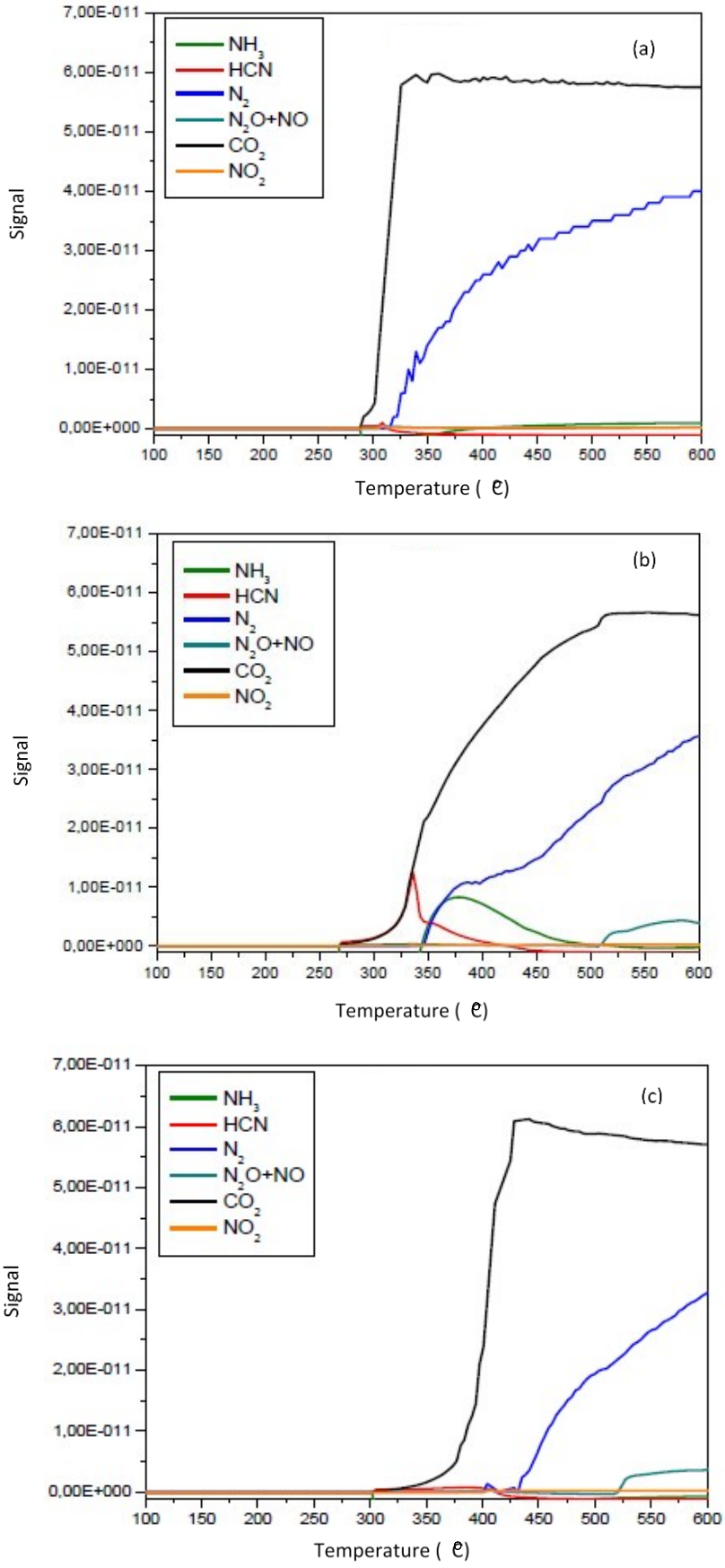

Figure 5: Products formed on the (a) Cu-Beta, (b) Fe- Beta and (c) Co-Beta catalysts.

4. CONCLUSION

The results showed the co-existence of Cu^{2+} exchanged and highly dispersed CuO nanoparticles in Cu-Beta. In Fe-Beta were identified octahedral Fe^{3+} ions and Fe_2O_3 nanoparticles. No cobalt oxide was observed in all analyses. However, cobalt ions exchanged have been suggested in Co-Beta, which means that it should only be reduced at high temperatures. On the other way, the reduction occurred in more than one step in the (Cu and Fe)-Beta catalysts. The acetonitrile conversion increased with increasing reaction temperature and the order of activity was Cu-Beta > Fe-Beta > Co-Beta. The results showed that Cu-Beta was the most active and with highest N_2 formation. The excellent performance of Cu-Beta was attributed to the co-existence of both highly dispersed CuO nanoparticles and Cu^{2+} species.

5. ACKNOWLEDGEMENTS

The authors would like to thank the CNPq - National Council for Scientific and Technological Development, the CAPES - Coordination for the Improvement of Higher Education Personnel and the FAPEMIG - Minas Gerais State Research Foundation for financial support (scholarships and research grants).

6. REFERENCES

1. Ren Y, Qu Z, Du Y, Xu R, Ma D, Yang G, et al. Air quality and health effects of biogenic volatile organic compounds emissions from urban green spaces and the mitigation strategies. Environ Pollut. 2017;230:849-61. doi: 10.1016/j.envpol.2017.06.049
2. He F, Jeon W, CHOI W. Photocatalytic air purification mimicking the self-cleaning process of the atmosphere. Nat Comm. 2021;12(1):1-4. doi: 10.1038/s41467-021-22839-0
3. Shan Y, Liu Y, Li Y, Yang W. A review on application of cerium-based oxides in gaseous pollutant purification. Sep Purif Technol. 2020;250:117181. doi: 10.1016/j.seppur.2020.117181
4. Zhang R, Liu N, Lei Z, Chen B. Selective transformation of various nitrogen-containing exhaust gases toward N_2 over zeolite catalysts. Chem Rev. 2016;116:3658-721. doi: 10.1021/acs.chemrev.5b00474
5. Johnson LD, Fuerst RG, Steger JL, Bursey JT. Evaluation of a sampling method for acetonitrile emissions from stationary sources. Proc EPA/A&WMA Int Symp: Meas Toxic Related Air Pollutants, Res Triangle Park. 1997;74:149-58.
6. Hanif NM, Hawari NSSL, Othman M, Abd Hamid HH, Ahamad F, Uning R, et al. Ambient volatile organic compounds in tropical environments: Potential sources, composition and impacts–A review. Chemosphere. 2021;131355. doi: 10.1016/j.chemosphere.2021.131355
7. Cao Y, Chen BH, Zhang, RD. Selectively Catalytic combustion of acetonitrile by transition-metal supported mesoporous molecular sieve SBA-15. Chem J Chin Univ. 2011;12:2849-55.
8. Alzueta MU, Guerrero M, Millera Á, Marshall P, Glarborg P. Experimental and kinetic modelling study of oxidation of acetonitrile. Proc Combustion Inst. 2021;38:575-83. doi: 10.1016/j.proci.2020.07.043
9. Kamal MS, Razzak SA, Hossain MM. Catalytic oxidation of volatile organic compounds (VOCs)–A review. Atmos Environ. 2016;140:117-34. doi: 10.1016/j.atmosenv.2016.05.031
10. Everaert K, Baeyens J. Catalytic combustion of volatile organic compounds. J Hazard Mater. 2004;109:113-39. doi: 10.1016/j.jhazmat.2004.03.019
11. Zhang R, Shi D, Liu N, Cao Y, Chen B. Mesoporous SBA-15 promoted by 3d-transition and noble metals for catalytic combustion of acetonitrile. Appl Catal B. 2014;146:79-93. doi: 10.1016/j.apcatb.2013.03.028
12. Nanba T, Masukawa S, Uchisawa J, Obuchi A. Screening of catalysts for acrylonitrile decomposition. Catal Lett. 2004;93:195-201. doi: 10.1023/B:CATL.0000017076.63005.56
13. Wang Y, Ying Q, Zhang Y, Liu Y, Wu Z. Reaction behaviours of CH3CN catalytic combustion over CuCeOx-HZSM-5 composite catalysts: The mechanism of enhanced N2 selectivity. Appl Catal A. 2020;590:117373. doi: 10.1016/j.apcata.2019.117373
14. Zhang Y, Wang Y, Liu Y, Ying Q, Wu Z. Catalytic combustion of acetonitrile over CuCeOx-HZSM-5 composite catalysts with different mass ratios: The synergism between oxidation and hydrolysis reactions. J Coll Int Sci. 2021;584:193-203. doi: 10.1016/j.jcis.2020.09.091
15. Sudarsanam P, Peeters E, Makshina EV, Parvulescu VI, Sels BF. Advances in porous and nanoscale catalysts for viable biomass conversion. Chem Soc Rev. 2019;48(8):2366-421. doi: 10.1039/C8CS00452H

16. Zhang K, Liu Z, Wang M, Yan X, Li C, Xi H. Synthesis and catalytic performance of hierarchically structured beta zeolites by a dual-functional templating approach. New J Chem. 2017;41(10):3950-56.
17. Van der Mynsbrugge J, Visur M, Olsbye U, Beato P, Bjørgen M, Van Speybroeck V, et al. Methylation of benzene by methanol: Single-site kinetics over H-ZSM-5 and H-beta zeolite catalysts. J Catal. 2012;292:201-12. doi: 10.1016/j.jcat.2012.05.015
18. Akah AC, Nkeng G, Garforth AA. The role of Al and strong acidity in the selective catalytic oxidation of NH3 over Fe-ZSM-5. Appl Catal B. 2007;74(1-2):34-9. doi: 10.1016/j.apcatb.2007.01.009
19. Zhang T, Liu J, Wang D, Zhao Z, Wei Y, Cheng K, et al. Selective catalytic reduction of NO with NH3 over HZSM-5-supported Fe–Cu nanocomposite catalysts: The Fe–Cu bimetallic effect. Appl Catal B. 2014;148:520-31. doi: 10.1016/j.apcatb.2013.11.006
20. Fauzi A, Ratnawulan R. The effect of calcination temperature on the structure of iron oxide phase from west Sumatra. J Phys: Conf Ser. 2021;1876(1):012028-35. doi: 10.1088/1742-6596/1876/1/012028
21. Aziz A, Sajjad M, Kim M, Kim KS. An efficient Co-ZSM-5 catalyst for the abatement of volatile organics in air: effect of the synthesis protocol. Int J Env Sci Tech. 2018;15(4):707-18. doi: 10.1007/s13762-017-1442-8
22. Jiang L, Sui Y, Qi J, Chang Y, He Y, Meng Q, et al. Structure dependence of Fe-Co hydroxides on Fe/Co ratio and their application for supercapacitors. Part Part Syst Char. 2017;34(2):1600239. doi: 10.1002/ppsc.201600239
23. Amaki E, Sahraei R. Preparation, characterization and optical properties of nanostructured undoped and Cu doped ZnO thin films. Bulgarian Chem Comm. 2016;48:131-7.
24. Quiton KG, Lu MC, Huang YH. Reclamation of cobalt and copper from single-and co-contaminated wastewater via carbonate and hydroxide precipitation. Res Square. 2021;1-36. doi: 10.21203/rs.3.rs-910544/v1
25. Jouini H, Mejri I, Petitto C, Martinez-Ortigosa J, Vidal-Moya A, Mhamdi M, et al. Characterization and NH_3-SCR reactivity of Cu-Fe-ZSM-5 catalysts prepared by solid state ion exchange: The metal exchange order effect. Micropor Mesopor Mater. 2018;260:217-26. doi: 10.1016/j.micromeso.2017.10.051
26. Rutkowska M, Chmielarz L, Macina D, Piwowarska Z, Dudek B, Adamski A, et al. Catalytic decomposition and reduction of N2O over micro-mesoporous materials containing Beta zeolite nanoparticles. Appl Catal B. 2014;146:112-22. doi: 10.1016/j.apcatb.2013.05.005
27. Liu N, Shi D, Zhang R, Li Y, Chen B. Highly selective catalytic combustion of acrylonitrile towards nitrogen over Cu-modified zeolites. Catal Today. 2019;332:201-13. doi: 10.1016/j.apcatb.2013.05.005Get rights and content
28. Blanch-Raga NEUS, Palomares AE, Martínez-Triguero J, Valencia S. Cu and Co modified Beta zeolite catalysts for the trichloroethylene oxidation. Appl Catal B. 2016;187:90-7. doi: 10.1016/j.apcatb.2016.01.029
29. Romero-Sáez M, Divakar D, Aranzabal A, González-Velasco JR, González-Marcos JA. Catalytic oxidation of trichloroethylene over Fe-ZSM-5: Influence of the preparation method on the iron species and the catalytic behavior. Appl Catal B. 2016;180:210-18. doi: 10.1016/j.apcatb.2015.06.027
30. Zhou H, Ge M, Zhao H, Wu S, Li M, Su Y. Selective Catalytic reduction of nitric oxide with propylene over Fe/Beta catalysts under lean-burn conditions. Catal. 2019;9(2):205. doi: 10.3390/catal9020205
31. Song S, Wu G, Dai W, Guan N, Li L. Al-free Fe-Beta as a robust catalyst for selective reduction of nitric oxide by ammonia. Catal Sci Tech. 2016;6(23):8325-35.
32. Biturini NF, Santos APN, Batista MS. Influence of co-fed gases (O_2, CO_2, CH_4, and H_2O) on the N_2O decomposition over (Co, Fe)-ZSM-5 and (Co, Fe)-BETA catalysts. Reac Kinet Mech Catal. 2019;126(1):341-52. doi: 10.1007/s11144-018-1506-x
33. Wang Y, Zhao W, Li Z, Wang H, Wu J, Li M, et al. Application of mesoporous ZSM-5 as a support for Fischer–Tropsch cobalt catalysts. J Porous Mater. 2015;22(2):339-45. doi: 10.1007/s10934-014-9901-9
34. Wang H, Xu R, Jin Y, Zhang R. Zeolite structure effects on Cu active center, SCR performance and stability of Cu-zeolite catalysts. Catal Today. 2019;327:295-307. doi: 10.1016/j.cattod.2018.04.035
35. Rutkowska M, Piwowarska Z, Micek E, Chmielarz L. Hierarchical Fe-, Cu-and Co-Beta zeolites obtained by mesotemplate-free method. Part I: Synthesis and catalytic activity in N_2O decomposition. Micropor Mesopor Mater. 2015;209:54-65. doi: 10.1016/j.micromeso.2014.10.011
36. Kim J, Jentys A, Maier SM, Lercher JA. Characterization of Fe-exchanged BEA zeolite under NH_3 selective catalytic reduction conditions. J Phys Chem C. 2013;117(2):986-93. doi: 10.1021/jp309277n
37. Chen HH, Shen SC, Chen X, Kawi S. Selective catalytic reduction of NO over Co/beta-zeolite: effects of synthesis condition of beta-zeolites, Co precursor, Co loading method and reductant. Appl Catal B. 2004;50(1):37-47. doi: 10.1016/j.apcatb.2003.10.005

38. Chen S, Yan X, Wang Y, Chen J, Pan D, Ma J, et al. Effect of SO_2 on Co sites for NO-SCR by CH_4 over Co-Beta. Catalysis Today. 2011;175(1):12-7. doi: 10.1016/j.cattod.2011.05.024
39. Silva PH, Oliveira HS, Batista MS. Redox effects in Cu, Co or Fe in oxides nanocrystals with high catalytic activity for the acetonitrile combustion. SN Applied Sciences. 2020;2(4):649. doi: 10.1007/s42452-020-2476-y
40. Zhang R, Shi D, Liu N, Chen B, Wu L, Wu L, et al. Catalytic purification of acrylonitrile-containing exhaust gases from petrochemical industry by metal-doped mesoporous zeolites. Catal Today. 2015;258:17-27. doi: 10.1016/j.cattod.2015.03.021
41. Zhang R, Hedjazi K, Chen B, Li Y, Lei Z, Liu N. M (Fe, Co)-BEA washcoated honeycomb cordierite for N_2O direct decomposition. Catal Today. 2016;273:273-85. doi: 10.1016/j.cattod.2016.03.021
42. Zhang Y, Wang Y, Liu Y, Ying Q, Wu Z. Catalytic combustion of acetonitrile over CuCeOx-HZSM-5 composite catalysts with different mass ratios: The synergism between oxidation and hydrolysis reactions. J Colloid Interface Sci. 2021;584:193-203. doi: 10.1016/j.jcis.2020.09.091
43. Wang Y, Ying Q, Zhang Y, Liu Y, Wu Z. Reaction behaviors of CH3CN catalytic combustion over CuCeOx-HZSM-5 composite catalysts: The mechanism of enhanced N2 selectivity. Appl Catal A. 2020;590:117373. doi: 10.1016/j.apcata.2019.117373